

Single-scan 2D NMR spectroscopy on a 25 T bitter magnet

Boaz Shapira ^a, Kiran Shetty ^b, William W. Brey ^b, Zhehong Gan ^b, Lucio Frydman ^{a,*}

^a *Department of Chemical Physics, Weizmann Institute of Science, 76100 Rehovot, Israel*

^b *National High Magnetic Field Laboratory, 1800 East, Paul Dirac Drive, Tallahassee, FL 32310, USA*

Received 27 March 2007; in final form 22 May 2007

Available online 8 June 2007

Abstract

2D NMR relies on monitoring systematic changes in the phases incurred by spin coherences as a function of an encoding time t_1 , whose value changes over the course of independent experiments. The intrinsic multi-scan nature of such protocols implies that resistive and/or hybrid magnets, capable of delivering the highest magnetic field strengths but possessing poor temporal stabilities, become unsuitable for 2D NMR acquisitions. It is here shown with a series of homo- and hetero-nuclear examples that such limitations can be bypassed using recently proposed 2D ‘ultrafast’ acquisition schemes, which correlate interactions along all spectral dimensions within a single-scan.

© 2007 Published by Elsevier B.V.

1. Introduction

The quest for operating at the highest possible magnetic field strength has been an integral part of the progress undergone by nuclear magnetic resonance (NMR) over its 60 year history [1]. Stronger magnetic fields benefit NMR’s sensitivity with an increase in the polarization to be measured and in the strength of the spin coherences’ inductive coupling, and they improve resolution owing to the linear field dependence that characterizes chemical shift dispersions [2]. High magnetic fields are also important components in a growing number of line-narrowing experiments based on transverse-optimized relaxation phenomena [3,4]. A significant leap in the strength (and quality) of the fields available for analytical NMR experiments occurred in the early seventies, with the dissemination of vertical-bore designs relying on solenoidal, superconductive-wires arrangements. Following an initial ‘burst phase’ in superconducting magnet design, however, only modest B_0 field increases have taken place over the ensuing years, with Nb-based technologies appearing to have reached full

potential at around 22 T magnetic field strengths. A number of alternatives are consequently being explored in an effort to supersede this limit, including a series of designs that couple resistive magnets incorporating ‘mega-currents’ in their field-forming elements [5–11]. These efforts have lead to the realization of NMR experiments at fields of 25 and 33 T on Bitter electromagnets [5–7], at 45 T in hybrid electro/superconducting magnets [8], and at fields approaching 70 T in pulsed-magnet experiments [9–11].

A feature that appears associated to operating in magnets that, like the ones just mentioned, are driven by currents running tens-of-thousands of Amperes, is a relatively high degree of field instability—at least by the usually exacting NMR standards. For example, in the 25 T Keck system operating at the US National High Magnetic Field Lab (NHMFL), which is the magnet forming the basis of the experiments reported in this study, the thermal and electrical stabilities of the DC power supplies operating this 19 MW unit can reduce fluctuations down to a few parts-per-million. NMR-wise, however, this still results in a ^1H resonance that drifts an average of ≈ 10 kHz/s from its central 1066 MHz Larmor frequency. This kind of drift can be tolerated and even compensated in single-scan one-dimensional (1D) NMR acquisitions by relying on deconvolution techniques that monitor, in addition to the desired

* Corresponding author. Fax: +972 8 9344123.

E-mail address: Lucio.Frydman@weizmann.ac.il (L. Frydman).

signals, an additional heteronuclear reference resonance [12]. But they preclude most procedures that rely on the averaging of multiple phase-coherent scans, including phase-cycling and a majority of two-dimensional (2D) NMR acquisitions [1,13]. Indeed the generic framework of 2D NMR requires that a series of time-domain signals $S(t_2)$ be collected as a function of a time delay t_1 , whose duration undergoes a parametric incrementation throughout independent experiments [14]. In a majority of cases a magnet that changes in an alleatory fashion will prevent one from monitoring the desired multi-scan t_1 evolution arising from the relevant spin interactions, as most modulations affecting spins over this period will become corrupted by an artificial t_1 -noise. A sole notable exception to this behavior arises when considering acquisitions focusing their t_1 evolution on zero-quantum differences between the chemical shifts of nearby sites; an experiment of this kind constitutes the only 2D NMR case hitherto reported from the NHMFL's Keck electromagnet [15]. For dealing with the implementation of other kinds of 2D NMR scenarios, this Letter discusses the potential opened up by the advent of ultrafast techniques when dealing with unstable, inhomogeneous magnetic fields of this sort.

2. Experimental setup

As mentioned, this research took place on the Keck resistive magnet sited at the NHMFL facility capable of generating a field of 25 T, corresponding to ^1H and ^{13}C Larmor frequencies of ca. 1066 and 268 MHz, respectively. This is an electromagnet of Bitter design that operates driven by 38.8 kA of DC current, stabilized to a precision better than 1 part in 100 000. While under operation the magnet dissipates its 19 MW heat flow into a constant supply of cooling water that runs through it at a 7000 L/min flow rate, raising the water temperature from 9 to 43 °C. The availability of a 5 000 000 L tank and water chiller allows continuing operation of the magnet at the full field strength ca. ≈ 10 hs before having to discontinue its operation. The magnet is equipped with custom-made ferroschims leaving a 52 mm internal bore, into which a custom-built high-resolution Doty Sci. double-resonance inverse probe equipped with a 90 G/cm single-axis z gradient (and ca. 50 μs gradient rise/fall times) was fitted. All experiments were written for and driven by a PC-based Tecmag Discovery[®] console; the overall setup resulted in minimum $\pi/2$ ^{13}C and ^1H pulses of 22 and 16.2 μs , respectively. Further characterizations of the magnet's homogeneity using the probe's z gradient and a Teflon phantom revealed a static field distribution of ≈ 2 kHz over a 5 mm region (Fig. 1A and B). Superimposed on this fairly constant inhomogeneity profile there was a ca. 2 kHz Larmor frequency fluctuation exhibiting a strong 60 Hz modulation ascribed to instabilities (ripples) in the magnet's DC power supply (Fig. 1C); a larger, longer-term overall drift reaching into the 10 s of kHz

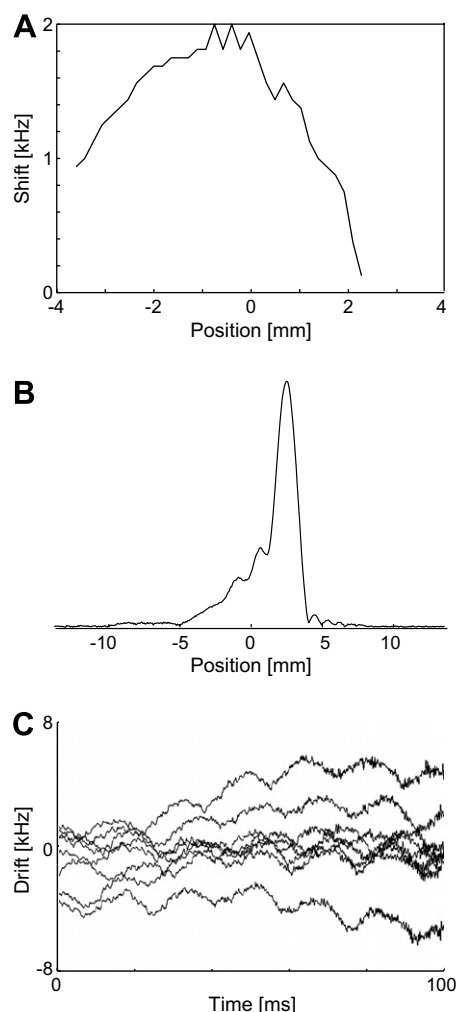


Fig. 1. Challenges posed by the NHMFL's 25 T Keck magnet to 2D NMR spectroscopy, as viewed by a single ^1H NMR tests carried out on a water sample on a high resolution probe incorporating a 5 mm diameter/10 mm long coil. (A) Instantaneous spatial profile observed as a function of sample position, arising from a gradient-echo sequence. (B) Another view of the inhomogeneity profile, translated into a frequency distribution. (C) Average shift displacement evidenced for the system as a function of time, as measured by the phases displayed by eight consecutive single-scan H_2O acquisitions. The oscillation within each trace reflects a 60 Hz frequency, while deviations between traces reflect the drift over a few seconds. On longer timescales (min) drifts in the 10 s of kHz can be measured; all drifts superimpose on the spatial inhomogeneity profile compounding the overall problem.

was also observed. Although field stabilization attempts based on the operation of pick-up coils were assayed and worked successfully in conventional single-pulse experiments, their operation in single-scan 2D acquisitions gave origin to sizable artifacts and was therefore discontinued. We presume that these originated in cross-talk phenomena between the pick-up coils and the probe's pulse field gradients; further refinements to compatibilize these two systems are being explored. We should add that whereas these fluctuations had minor effects in the overall spatial profiles of the magnetic field, field inhomogeneities varied between different experimental sessions.

3. Results

In view of the inhomogeneities and instabilities just mentioned, the Keck magnet presents a considerable challenge towards the acquisition of conventional 2D NMR spectra. To alleviate this limitation we thought it convenient to assay the implementation of different 2D NMR acquisitions schemes based on the recently developed single-scan ‘ultrafast’ 2D NMR protocol. As explained elsewhere [16,17] this approach replaces the traditional t_1 time-encoding by a $C\Omega_1(z - z_0)$ spatial winding, imparted via refocused magnetic field gradients G_e acting in synchrony with frequency-swept radiofrequency (RF) pulses. The $I(\Omega_1)$ spectrum encoded by such spatial pattern is then repeatedly read out by oscillating an acquisition gradient G_a during each Δt_2 ; the gradient echoes arising during each such dwell time can then be Fourier transformed as a function of the direct-domain acquisition time t_2 , to provide the 2D $I(\Omega_1, \Omega_2)$ NMR spectrum being sought. A variety of spatial encoding modes discussed in the literature were assayed over the course of this study, including discrete and continuous excitations as well as real-time and constant time alternatives [17–20]. Only those modes that displayed the best experimental performance are hereby presented.

Fig. 2 shows representative 2D ^1H – ^{13}C correlation results obtained on this system, using ^{13}C -enriched glycerol in H_2O as test sample. Shown in panel (A) is the sequence used in this heteronuclear correlation; it is a constant-time HSQC protocol, which ended up given an improved performance *vis-à-vis* competing heteronuclear correlation alternatives. We presume that HSQC ended up performing better than HMQC counterparts because of the former’s higher immunity against field inhomogeneities and instabilities, and that a constant-time operation lead in this case to better results than real-time acquisitions because of the shorter encoding times that it involved. Although all these tests had to be implemented on a single-scan basis, quality background-free single-scan 2D data could be retrieved thanks to the coherence selection abilities of the various field gradient filters involved.

Dominating the FID shapes observed in these experiments as a function of t_2 is a sizable modulation of the signal’s envelop (Fig. 2B), reflecting the refocusing of the B_0 inhomogeneities undergone by the spins during the indirect-domain evolution and following the $^{13}\text{C} \rightarrow ^1\text{H}$ coherence transfer. Indeed, the ^1H signal that is observed in the direct-domain shows a strong dependence in both its amplitude and timing on the values chosen for the duration of the ^{13}C encoding. This echoing behavior results in a signal that is considerably longer-lived than its single-pulse counterpart, and thereby in an increase in the spectral resolution along the direct dimension. Unfortunately, given the parameters that were available, particularly the field gradient G_a which when multiplied by the direct-domain

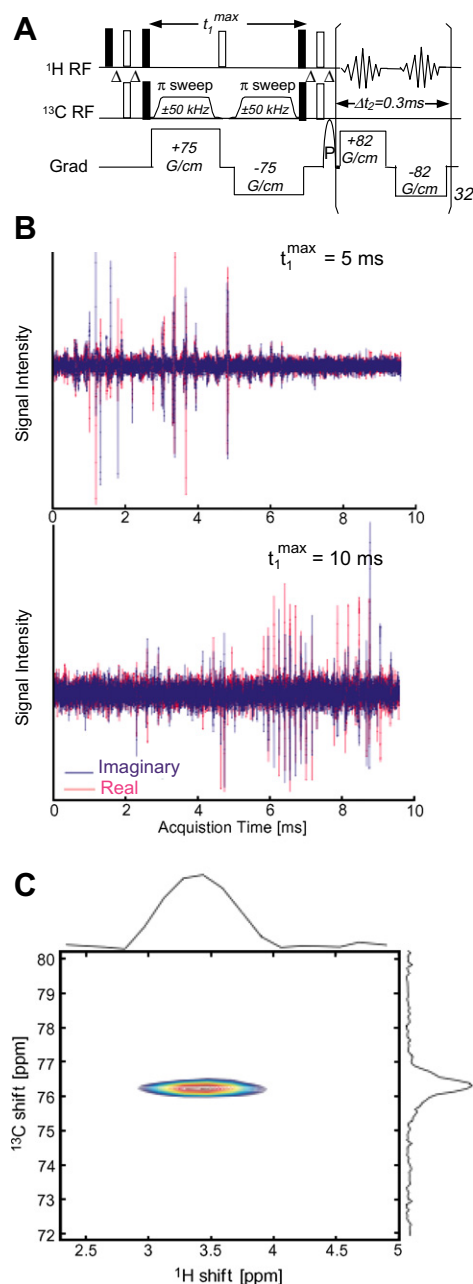


Fig. 2. Representative heteronuclear correlation results obtained on a D_2O solution of $^{13}\text{C}_3$ -glycerol on the 25 T Keck magnet. (A) Sequence and parameters employed in the single-scan 2D acquisition, with full and hollow bars corresponding to $\pi/2$ and π pulses and $\Delta = 1.69$ ms (corresponding to $4J_{\text{CH}}^{-1}$). The acquisition took place at a 1 MHz digitization rate, P is a $100 \mu\text{s}$ long purging gradient pulse. (B) Characteristic time-domain signals showing an overall envelop that peaks at ca. $2\gamma_{\text{C}}t_1^{\text{max}}/\gamma_{\text{H}}$ and reflecting a refocusing of inhomogeneities by the $^{13}\text{C} \rightarrow ^1\text{H}$ coherence echo in the 2D sequence. Each sharp echo within these time-domain signals corresponds to an indirect-domain ^{13}C spectrum, to be rearranged and Fourier transformed along t_2 to reveal the proper ^1H correlations [16]. Deviations in the exact timing of the envelop maxima are ascribed to drifts of the magnet. (C) Single-scan 2D ^{13}C – ^1H NMR correlation arising from imposing such processing on the $t_1^{\text{max}} = 10$ ms data set, incorporating cross sections of the data along the direct and indirect-domains and referenced so as to fit literature data [21]. Notice the different dimensions (in ppm) of the two spectral axis.

^1H dwell time Δt_2 defines the spectral width accessible in the indirect dimension, we were unable to fit the multiple ^{13}C sites within each single-scan acquisition. The overall encoding time t_1^{max} was thus chosen at ca. 5–10 ms so as to optimize the methylene signal, which is in turn considerably more intense than that of its methine counterpart. (Notice that under conventional high-resolution conditions a longer evolution time, e.g. 25 ms, allows observation of both ^{13}C sites in the molecule with good intensities; yet the strong 60 Hz fluctuations in the Keck magnet were found to impart severe signal losses upon employing such long evolution times.) Similar Δt_2 constraints forced us to work without ^{13}C decoupling π -pulses; this may be the reason that slightly larger linewidths (≈ 0.2 in ppm) were observed along the direct than along the indirect spectral dimensions. Fig. 2C illustrates the kind of heteronuclear correlations that for this site could then be typically observed.

In addition to these heteronuclear correlations a variety of homonuclear ^1H – ^1H 2D sequences were also assayed. These confront amplified stability problems *vis-à-vis* their heteronuclear counterparts because of the larger γ 's and smaller shift dispersions involved; they are further challenged by the weaker J -couplings and thereby longer coherence transfer times required. Extensive tests showed that best results were observed in this kind of correlations upon relying on a real-time spatial encoding based on the application of two consecutive $\pi/2$ pulses, rather than on the constant-time approach described above. In addition to its spatial encoding abilities, this excite/store combination provided us with a suitable starting point for the correction of field inhomogeneities, based on the 'RF shimming' protocol. As explained elsewhere in further detail [22–24] this kind of corrections operate based on an *a priori* mapping of the field distribution along the encoding z axis, followed by the addition of suitable RF-imposed phase shifts that account for the effect of field distortions at the time of the data acquisition. The results of assaying such procedure on an ethanol sample are shown in Fig. 3, and evidence a substantial narrowing *vis-à-vis* the line widths that characterized the ^1H spectra in single-pulse experiments. The line-narrowing introduced by this form of 'RF shimming', coupled to a correlation of transverse broadenings along the two spectral domains akin to the one described for the heteronuclear case, enables a resolution of chemically inequivalent sites that is simply unavailable in the 1D spectrum. Following this set of initial promising results a variety of homonuclear mixing variants were assayed, but they all exhibited prohibitive signal losses even if relying on a variety of optimized π -trains, which made the observation of the putative cross peaks difficult to ascertain. Further efforts to make these mixing processes more resilient to field instabilities and heterogeneities are under way.

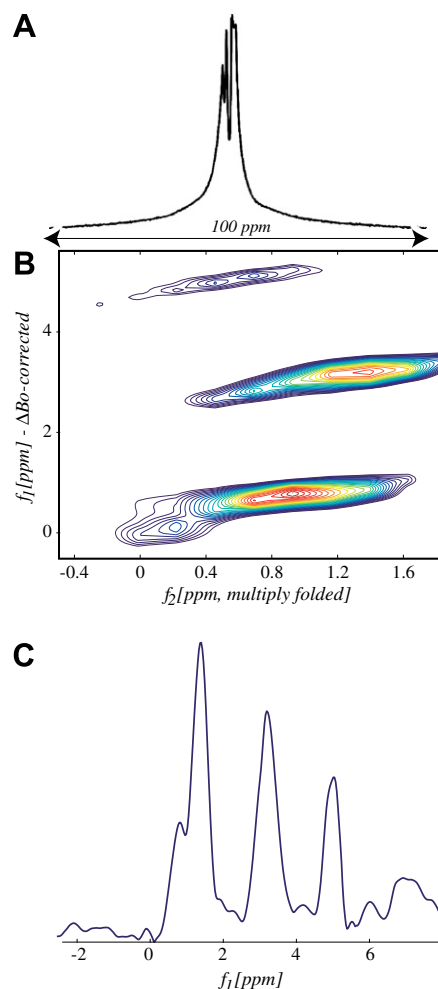


Fig. 3. Features associated to homonuclear ultrafast 2D NMR acquisitions in the Keck magnet. (A) 1D NMR trace arising from an ethanol sample after a single pulse excitation. (B) Mixing-less single-scan ^1H 2D NMR spectrum incorporating a $t_1^{\text{max}} = 3$ ms, 0.46 ms Δt_2 dwell time, excitation and acquisition gradients $G_c = 80$, $G_a = 90$ G/cm, and excitation/storage $\pi/2$ pulses sweeping ± 105 kHz and incorporating a compensation of the axial field inhomogeneities that, based on the field maps shown in Fig. 1, operate as described in Ref. [22]. Notice the slight slanting of the peaks arising from each inequivalent site, which we ascribe to the coherence echoing of the residual field inhomogeneities. (C) Slice extracted from the experimental 2D spectrum, showing a nearly 10-fold resolution enhancement *vis-à-vis* the single-pulse trace and a potential for resolving various sites. Spectral axes in (B) and (C) are in ppm and were referenced externally to H_2O .

4. Discussion and conclusions

Incorporating non-superconducting elements into magnetic setups could open up exciting new avenues in high-field NMR. Although spatial inhomogeneities and temporal instabilities are integral characteristics of such elements, spatial encoding approaches of the kind detailed here could alleviate the influence of these drawbacks when considering the acquisition of 2D NMR data. Indeed the single-scan possibilities opened up by the spatial encoding

approaches, though still evidently at a preliminary stage, bode well for the collection of homo- and hetero-nuclear 2D spectral data. This potential includes the possibility to signal average in the frequency domain multiple single-transient absolute value data sets of the kind originating the correlation plot in Fig. 2C, and field inhomogeneity compensation procedures of the kind illustrated in Fig. 3. Still, it is clear that extensive improvements are needed for making this kind of experiments practical on an every-day basis. Achieving a better temporal stability, for instance by improving the compatibility of field stabilizing and pulsed field gradient setups, would be one of the first steps needed for facilitating an implementation of the relatively long mixing processes required by homonuclear correlations. Rapid mechanical spinning of the sample, if made compatible with the use of field gradients, could also aid significantly in reducing the rapid decay arising from radial inhomogeneities. And developing 2D pulse sequences that encode differences between the sites' instantaneous chemical shifts rather than their absolute values [25], could also go a long way in aiding to the implementation of homonuclear correlations in such intrinsically heterogeneous systems. These and other experimental approaches are currently being explored, with the aim of making this kind of experiments more accessible.

Acknowledgements

We are grateful to Drs. Bruce Brandt and Peter Gor'kov (NHMFL) for their support and help in this project. This work was supported by the Israel Science Foundation (ISF 1206/05), by the US National Institutes of Health (GM-72565), and by the National High Magnetic Field Laboratory through the US National Science Foundation and the State of Florida Cooperative Agreement DMR0084173.

References

- [1] J.W. Emsley, J. Feeney, *Prog. Nucl. Mag. Reson. Spectrosc.* 28 (1995) 1.
- [2] E. Becker, *High Resolution NMR*, Academic Press, New York, 2000.
- [3] K. Pervushin, R. Riek, G. Wider, K. Wüthrich, *Proc. Natl. Acad. Sci. USA* 94 (1997) 12366.
- [4] D.M. Korzhnev, K. Kloiber, V. Kanelis, V. Tugarinov, L.E. Kay, *J. Am. Chem. Soc.* 126 (2004) 3964.
- [5] M.D. Bird, S. Bole, Y.M. Eyssa, Z. Gan, *IEEE Trans. Appl. Supercond.* 10 (2000) 443.
- [6] P.J.M. van Bentum, J.C. Maan, J.W.M. van Os, A.P.M. Kentgens, *Chem. Phys. Lett.* 376 (2003) 338.
- [7] A. Samoson, T. Tuherm, *Z. Gan, Solid State Nucl. Mag. Reson.* 20 (2001) 130.
- [8] Z. Gan, P. Gor'kov, T.A. Cross, A. Samoson, D. Massiot, *J. Am. Chem. Soc.* 124 (2002) 5634.
- [9] J. Haase, M. Kozlov, K.-H. Müller, H. Siegel, B. Büchner, H. Eschrig, A.G. Webb, *J. Magn. Mater.* 290 (2005) 438.
- [10] M. Kozlov, J. Haase, C. Baumann, A.G. Webb, *Solid State Nucl. Mag. Reson.* 28 (2005) 64.
- [11] J. Haase, *Solid State Nucl. Mag. Reson.* 27 (2005) 206.
- [12] Z. Gan et al., in: 44th Experimental NMR Conference, Savannah, GA, March 2003.
- [13] R.R. Ernst, G. Bodenhausen, A. Wokaun, *Principles of Nuclear Magnetic Resonance in One and Two Dimensions*, Clarendon, Oxford, 1987.
- [14] W.P. Aue, E. Bartholdi, R.R. Ernst, *J. Chem. Phys.* 64 (1976) 2229.
- [15] Y.-Y. Lin, S. Ahn, N. Murali, W.W. Brey, C.R. Bowers, W.S. Warren, *Phys. Rev. Lett.* 85 (2000) 3732.
- [16] L. Frydman, T. Scherf, A. Lupulescu, *Proc. Natl. Acad. Sci. USA* 99 (2002) 15858.
- [17] L. Frydman, *Compt. Rends. Chimie* 9 (2006) 336.
- [18] L. Frydman, T. Scherf, A. Lupulescu, *J. Am. Chem. Soc.* 125 (2003) 9204.
- [19] P. Pelupessy, *J. Am. Chem. Soc.* 125 (2003) 12345.
- [20] Y. Shrot, B. Shapira, L. Frydman, *J. Magn. Reson.* 171 (2004) 162.
- [21] See for instance Spectral Database For Organic Compounds at <<http://www.aist.go.jp/RIODB/SDBS/>>.
- [22] B. Shapira, L. Frydman, *J. Am. Chem. Soc.* 126 (2004) 7184.
- [23] D. Topgaard, R.W. Martin, D. Sakellariou, C.A. Meriles, A. Pines, *Proc. Natl. Acad. Sci. USA* 101 (2004) 17576.
- [24] B. Shapira, L. Frydman, *J. Magn. Reson.* 182 (2006) 12.
- [25] K. Nagayama, A. Kumar, K. Wüthrich, R.R. Ernst, *J. Magn. Reson.* 40 (1980) 321.